



Universidad Autónoma
de Madrid

Biblos-e Archivo
Repositorio Institucional UAM

Repositorio Institucional de la Universidad Autónoma de Madrid

<https://repositorio.uam.es>

Esta es la **versión de autor** del artículo publicado en:

This is an **author produced version** of a paper published in:

Journal of Plant Physiology 246-247 (2020): 153114

DOI: <https://doi.org/10.1016/j.jplph.2020.153114>

Copyright: © 2020 Elsevier Gm. This manuscript version is made available under the CC-BY-NC-ND 4.0 licence <http://creativecommons.org/licenses/by-nc-nd/4.0/>

El acceso a la versión del editor puede requerir la suscripción del recurso

Access to the published version may require subscription

Aluminium triggers oxidative stress and antioxidant response in the microalgae *Scenedesmus* sp

Maryam Ameri^{1*}, Angel Baron-Sola², Ramazan Ali Khavari-Nejad^{1,3}, Neda Soltani⁴, Farzaneh Najafi¹, Abdolreza Bagheri⁵, Flor Martinez², and Luis E. Hernández^{2*}

¹Department of Plant Science, Faculty of Biological Science, Kharazmi University, Tehran, Iran.

²Laboratory of Plant Physiology-Department of Biology/Research Centre for Biodiversity and Global Change, Universidad Autónoma Madrid, Darwin 2, ES28049 Madrid, Spain.

³Department of Biology, Science and Research Branch, Islamic Azad University, Tehran, Iran.

⁴Department of Petroleum Microbiology, Research Institute of Applied Science, ACECR, Tehran, Iran.

⁵Faculty of Agriculture, Ferdowsi University of Mashhad, Khorasan, Iran.

*Corresponding authors Email: ma.ameri65@gmail.com and luise.hernandez@uam.es

HIGHLIGHTS

- Aluminium (Al) induced oxidative stress in *Scenedesmus obliquus* algae after 72 h of exposure.
- Cells aggregated and suffer ultrastructural changes induced by Al.
- Changes in lipid metabolism and degradation of cellular organelles occurred under Al stress.
- Antioxidant enzymatic activity was compromised by Al, possibly leading to oxidative stress.
- Catalase was particularly sensitive to Al, enzyme that is envisaged as biomarker of Al toxicity.

Abstract

Aluminium (Al) water pollution is an increasing environmental problem and comprehensive analysis of toxic responses of aquatic primary producer organisms is imperative. We characterized the antioxidant response of *Scenedesmus* sp. microalga to Al-induced oxidative stress. After 72 h of exposure to Al (0, 10, and 100 μ M) in a modified Bold Basal Medium (pH 5.0), we observed cell aggregation and alterations in the subcellular structure, strong lipid peroxidation and oxidative stress induction (detected with the fluorescent probe 2',7'-dichlorodihydrofluorescein diacetate) in parallel with Al accumulation in cells. At the same time, Al toxicity caused depletion of important macronutrients like Ca, which is important for cell-wall structure. Analysis of antioxidant

enzymatic activities in Al-treated *Scenedesmus* cells revealed that catalase, ascorbate peroxidase, as well as different isoforms of superoxide dismutase were inhibited especially at the highest Al dose (100 μ M), cells that accumulated the highest concentration of Al. On the other hand, glutathione reductase activity increased at that Al concentration. Immunodetection after Western-blotting confirmed that only ascorbate peroxidase inhibition was apparently due to a decrease in enzyme levels. However, the inhibition of catalase and activation of glutathione reductase activities seemed related with post-translational modifications in protein function as protein expression decreased or increased, respectively under Al stress. Our results may help to understand toxic mechanisms triggered by Al in freshwater microalgae, which in turn could aid to select suitable biomarkers of Al contamination in aquatic ecosystems.

Keywords: aluminium, antioxidant enzymes, microalga, oxidative stress, *Scenedesmus* sp.

1. Introduction

Ongoing urbanization and industrialization in many countries lead to contamination of numerous aquatic ecosystems, frequently through uncontrolled discharges of wastewater loaded with relatively large amounts of toxic metals (Kumar et al., 2015). A major environmental burden is the retrieval of inorganic and organic loads of wastewaters by appropriate treatments to minimize the impact caused by those pollutants (Oller et al., 2011). Among different possibilities, bioremediation with photosynthetic organisms such as microalgae, which can generate a wide range of valuable products, provide the means of assimilating and metabolizing pollutants from wastewater (Christenson and Sims, 2011), while microalgal biomass production using wastewater can be attractive from both economic and environmental perspectives, since these organisms act as toxic metal bio-sorbents to clean contaminated effluents (Rugini et al., 2017).

Success in using microalgae to clean up wastewater depends highly on their tolerance to hazardous metals, which bind to cell walls and cytoplasmic biomolecules, resulting in their accumulation in several organelles and cellular compartments (Perales-Vela et al., 2006). Some pollutant metals are micronutrients essential for algal metabolism (i.e. Zn, Mn, Cu, or Fe) (Volland et al., 2011), and are normally hazardous at high concentrations (Miazek et al., 2015). However, metals like cadmium (Cd), lead (Pb), chromium (Cr) or mercury (Hg) are toxic even at relatively

low doses, hampering metabolism and microalgae growth (Kumar et al., 2015; Kováčik et al. 2018). In addition to growth inhibition and failure of important metabolic processes like photosynthesis and respiration, a typical symptom of metal toxicity is the induction of oxidative stress caused by imbalanced level of reactive oxygen species (ROS) (Okamoto et al., 2001; Kováčik et al. 2015). To counteract excessive levels of ROS induced by metals, microalgae possess a complex antioxidant system, comprised of several redox enzymes, such as superoxide dismutase (SOD), catalase (CAT), glutathione peroxidase (GPX), ascorbate peroxidase (APX), or glutathione reductase (GR), and reducing metabolites such as glutathione (GSH), ascorbate, β -carotene, or tocopherols (Foyer and Noctor, 2005). For example, Cd promoted the accumulation of reduced GSH in *Scenedesmus acutus* (Torricelli et al., 2004), and *Chlamydomonas reinhardtii* (Howe and Merchant, 1992), and promoted higher CAT and GR activities at the time that SOD activity decreased in *Scenedesmus acutiformis* (Kováčik et al. 2017). On the other hand, higher SOD activity appeared in *Spirulina platensis* treated with Zn, Cu and Pb (Choudhary et al., 2007).

Aluminium (Al) constitutes a large portion of Earth crust (up to 8%) mostly found as aluminium-silicate stable minerals, such as feldspar and clay, but due to anthropogenic acidification of soils it mobilises and eventually lixivates into adjacent water ecosystems (Bache, 1986). On the other hand, Portland cement manufacturing causes massive kiln dust deposition in areas surrounding these factories (Huntzinger and Eatmon, 2009), which contains Al oxides and silicates that can be released upon weathering (Siddique, 2006), as found in the Mashhad industrial site in Iran (Avami and Sattari, 2007). Tannery factories also contribute to increased release of soluble Al in the environment, because Al-hydroxides are used to adsorb and flocculate organic and metalliferous contaminants of wastewaters (Haydar and Aziz, 2009), carrying over relevant levels of residual Al (Gao et al. 2004). Thus, relatively high levels of Al occurred in reclaimed wastewater in Mashhad neighbouring sites that may represent a threat to consumers of local irrigated crop plants (Mousavi et al. 2013).

Aluminium chemical speciation is complex, and strongly depends on pH and salts concentration, forming aggregates generally at alkaline conditions, property used to withdraw suspended particles in treated waters (Hu et al., 2006). Nevertheless, there are several soluble forms of Al in aqueous soil solutions at acidic and neutral pH, such as Al^{3+} , $\text{Al}(\text{OH})_4^-$, and soluble Al-orthophosphate (AlHPO_4^+), which are bioavailable and cause numerous toxic effects in plants that lead to poor biomass and grain production (Sloan et al. 1995; Huynh et al., 2012). Among

them, Al impairs severely cell division and elongation at the root meristem (Delhaize and Ryan, 1995), interferes with the uptake of essential cationic metals, such as Ca^{2+} and Fe^{3+} (Lee et al., 2004), and alters membrane and cell wall integrity (Poschenrieder et al., 2008). Part of these toxic effects may correspond to the ability of Al to bind phospholipids, nucleotides and amino acid residues, resulting in the inhibition of H^+ -ATPase activity and membrane transporters (Ma, 2007). In parallel, Al affects the cellular redox balance, targeting mitochondria for ROS generation (Yamamoto et al., 2002), resulting in rapid accumulation of H_2O_2 at the root epidermis and induction of membrane lipid peroxidation (Jones et al. 2006).

Despite the ample literature describing the toxic effects of Al in plants, little is known about the mechanisms of toxicity triggered in microalgae. For example, Danilov et al. (2002) reported that AlCl_3 seriously impaired photochemical efficiency and oxygen evolution in *Euglena gracilis* cells. In addition, Al led accumulation of ROS, oxidative stress and activation of antioxidant defences in *Anabaena laxa* and *Nostoc muscorum* filamentous cyanobacteria (Hamed et al., 2019). However, there is scarce information with regards to the oxidative damage caused by Al in microalgae and how different antioxidant enzymes, such as CAT, SOD, GR, and APX, respond. Therefore, we studied the behaviour of a *Scenedesmus* sp. strain isolated from a pond storing wastewaters from the industrial area of Mashhad (Jorasán Razaví, Northeast Iran), which contains relatively high concentrations of Al. Our study may help to characterise physiological parameters readily sensitive to Al-induced toxicity, which could bring some light on the toxicity mechanisms triggered by Al in microalgae. Such knowledge would aid to select in future tolerant microalgae strains suitable for bioremediation of reclaimed industrial wastewater loaded with soluble Al, which is used currently for crop irrigation in arid countries like Iran.

2. Materials and methods

2.1. Microalgae and culture conditions

Scenedesmus sp. was isolated from an industrial area of Mashhad, and kept at the algal collection of the Research Institute of Applied Science of Academic Center for Education, Culture and Research (Tehran, Iran). Microalgae grew in 100 mL Erlenmeyer flasks under 16/8 light/dark illumination cycle with a photon flux of $20 \mu\text{mol m}^{-2}\text{s}^{-1}$, in 50 mL of Bold Basal Medium (BBM) [2.94 mM NaNO_3 , 0.17 mM CaCl_2 , 0.3 mM MgSO_4 , 0.43 mM K_2HPO_4 , 1.29 mM KH_2PO_4 , 17.1 mM EDTA, 55.3 mM KOH, 179 μM FeSO_4 , 18.50 μM H_3BO_3 , 0.31 μM ZnSO_4 , 7.28 μM MnCl_2 , 4.93 μM MoO_3 , 6.29 μM CuSO_4 , 1.68 μM $\text{Co}(\text{NO}_3)_2 \cdot 6\text{H}_2\text{O}$] at pH 6.8 (Bold 1949). Chemical

speciation of Al is particularly complex in the presence of inorganic and organic salts, which depends highly on medium pH (Sloan et al., 1995). We analysed *in silico* soluble chemical species of Al in BBM at pH 5.0 and 8.0 by means of Visual MINTEQ (V3.1) (Gustafsson, 2014). Table 1 shows pronounced differences of Al-soluble species, which depends on the Fe-chelating reagent used in BBM, either EDTA (ethylenediaminetetraacetic acid), or EDDHA (ethylenediamine-N, N'-bis (2-hydroxyphenylacetic acid)). In the absence of EDTA at pH 5.0, over 95% soluble Al was found as AlHPO_4^+ , and virtually all Al was found as $\text{Al}(\text{OH})_4^-$ at pH 8.0, so subsequently we used EDDHA to prepare a modified BBM when microalgae were exposed to Al. Acidic microalgae *Scenedesmus* sp. grew at similar rates at pH 5.0 or 8.0 (Fig. 1A), thus further experiments were performed in three times diluted BBM (BBM/3) containing EDDHA at pH 5.0, to ensure sufficient bioavailability of inorganic Al. Cells grew at exponential growth phase in conventional BBM (at pH 6.8), cells were subsequently centrifuged (3500 x g for 10 min), washed with BBM/3 and sub-cultured in 50 mL BBM/3 aliquots at pH 5.0 to an optical density (750 nm) between 0.15-0.2, and left to acclimate 24 h. Thereafter, Al was added at three different concentrations: 0, 10, and 100 μM (AlCl_3). *Scenedesmus* grew for 72 h and cells were collected by centrifugation (3500 x g for 10 min). Aliquots were prepared, snap-frozen in liquid nitrogen and kept at -80°C until analysis.

2.2. Chlorophyll concentration, lipid peroxidation and oxidative stress detection

Chlorophyll was quantified spectrophotometrically measuring absorbance at 665 and 650 nm, after extraction with absolute cold methanol (Fischer et al., 2006). For lipid peroxidation analysis, cells were homogenized using a mortar with 1 mL reaction mixture (15% (w/v) trichloroacetic acid, 0.37% (w/v) 2-tiobarbituric acid, and 0.25 M HCl), heated at 90°C for 30 min and centrifuged (12.000 x g, 15 min at 4°C). Absorbance measured at 535 nm and 600 nm was used for malondialdehyde determination (Ortega-Villasante et al., 2005).

Intracellular oxidative stress was detected by oxidation of the fluorogenic dye 2,7-dichlorofluorescein diacetate (H_2DCFDA), which reacts with ROS derived oxidants (Ortega-Villasante et al., 2016). 180 μL of cells (eight replicates per treatment), growing in BBM/3 supplemented with Al to OD_{750} between 0.1 and 0.2, were placed in a black 96-well microtiter plate. 20 μL of 200 μM H_2DCFDA in MiliQ H_2O were added, left to stabilize for 5 min, and fluorescence was read continuously for 60 min at 520 nm, excited at 485 nm (Synergy HT Reader, BioTek, Winooski, VT, USA).

2.3. Accumulation of Al and metals in cells

Approximately 100 mg of dehydrated cell pellet (dried in an oven at 50°C for 72 h) were transferred to chromatographic vial sealed with Teflon stoppers. Then, cells were digested in 1 mL of oxidative acidic mixture (HNO₃:H₂O₂:H₂O; 0.6:0.4:1, v:v) at 120°C and 1.5 atm for 30 min using an autoclave (Presoclave-75 Selecta, Barcelona, Spain) (Ortega-Villasante et al., 2005). Digests were diluted with MiliQ water to 5 mL, and Al, Ca, Mg, Fe and Zn were quantified in an ICP-MS NexION 300 (Perkin-Elmer Sciex, San Jose, CA, USA) at the Interdepartmental Research Service-UAM (SIDI). Analytical Relative Standard Deviation (RSD) was lower than 5%, and Limit of Detection (LOD) was adjusted by preliminary semi-quantitative analysis, usually set below the µg/L range.

2.4. Visible and transmission electron microscopy

Phase contrast microscopic images were obtained of cell suspensions and chlorophyll autofluorescence was collected to discriminate chloroplasts of microalgae cells from other particulate material, both using a motorized epifluorescence microscope (Olympus BX-61, Shinjuku, Japan). For transmission electron microscopy (TEM) visualization, 50 mL culture was centrifuged at 3500 x g for 5 min, and the pellet was washed twice with cold Sorensen's phosphate buffer pH 7.2. Cells were centrifuged again and fixed with glutaraldehyde 3.2% (v/v) in Sorensen's buffer during 3 h at 4°C (Ramazanov et al., 1994). After fixation, cells were centrifuged, washed twice again, and imbedded in bacteriological agar 2% (w/v) in Sorensen's buffer. Agar blocks were cut with a razorblade and incubated with osmium tetroxide 1% (w/v) in Sorensen's buffer for 2 h at 4°C. Blocks dehydrated by incubation in increasing ethanol concentrations from 30 to 100% (v/v), were embedded in Spurr epoxy resin (Electron Microscopy Sciences Ref. 14300, Hatfield, PA, USA), following the manufacturer's instructions. Once specimens polymerized during 24 h at 70°C, 50 nm sections were prepared using an ultramicrotome (Leica Reichert, Ultracut S, Germany) and placed over cooper grids. Sections were stained with 2% uranyl acetate for 5 min, and finally were counterstained for 45 s with 2% lead citrate, before visualization with a TEM 1200EX (JEOL USA Inc., Peabody, MA, USA).

2.5. Protein extraction and quantification

Protein was extracted from frozen algal biomass (0.5 g per mL of extraction buffer), with three series of freeze-thawing cycles, using liquid nitrogen to disrupt cells with a pestle and mortar. Cells

were mixed with the extraction buffer [30 mM 3-(N-morpholino) propanesulfonic acid (MOPS) at pH 7.3, 5 mM Na-EDTA, 10 mM dithiothreitol (DTT), 0.6% polyvinylpyrrolidone (PVP), 10 mM ascorbic acid, 1.5 mM phenyl methyl sulfonyl fluoride, and cocktail protease inhibitor (Ref. P2714, Sigma-Aldrich, St. Louis, MO, USA)]. Prior to use, protein concentration was determined with the BioRad Protein Assay reagent (Hercules, CA, USA), and the final loading for activity staining was adjusted after denaturing polyacrylamide gel electrophoresis (PAGE) and Coomassie-blue staining (Laemmli, 1970).

2.6. Redox enzymatic activity

Determination of redox enzymatic activity *in gel*, after separation of proteins by non-denaturing polyacrylamide gel electrophoresis (ND-PAGE), allows detection of changes in particular isoforms, and reduces artefacts that may appear of enzymatic activity measured *in vitro* in raw protein extracts. We used the procedures described by Sobrino-Plata et al. (2009) with minor modifications. Polyacrylamide concentration was 8% for CAT, and 10% for SOD, APX and GR, for appropriate resolution of activity bands. Protein amount ranged 10 to 20 μ g depending on the tested enzymes. CAT *in gel* activity was visualized as achromatic bands, firstly by incubating ND-PAGE in 3.3 mM H₂O₂ for 20 min, and by incubating with staining solution (1% (w/v) potassium ferric cyanide and 1% (w/v) ferric chloride). APX activity was detected in ND-PAGE gels loaded with 2 mM ascorbic acid, by a three-step incubation: firstly, gel slabs were submerged in 50 mM K-phosphate buffer at pH 7.0 containing 2 mM ascorbic acid. Secondly, were incubated in a reaction buffer composed of 4 mM ascorbic acid and 2 mM H₂O₂ 50 mM K-phosphate buffer at pH 7.0. Finally, achromatic APX activity band were revealed by transferring the gels to a 50 mM K-phosphate buffer (pH 7.8) containing 0.5 mM nitroblue tetrazolium (NBT) and 28 mM TEMED. SOD enzymatic activity was visualized after incubating the gels with 1.25 mM NBT in 50 mM Na-phosphate buffer at pH 7.8, with O₂^{•-} produced by the photooxidative reaction of 50 μ M riboflavine. MnSOD, FeSODs and Cu/ZnSODs isoforms were identified by their specific resistance to H₂O₂ and KCN (Beauchamp and Fridovich, 1971). For GR visualization, gels were dipped in 25 mM Tris-HCl buffer (pH 7.5) containing 3.4 mM oxidized glutathione (GSSG), 0.5 mM NADPH, 0.2 mg·mL⁻¹ 3-(4,5-dimethylthiazol-2-yl)-2,5-diphenyltetrazolium bromide, and 0.2 mg·mL⁻¹ dichlorophenol indophenol. Genuine GR activity bands were confirmed by assaying a parallel gel in the absence of GSSG to discriminate diaphorase activity (Sobrino-Plata et al.,

2009). At least three different gels were analysed for each enzymatic activity, and by means of data consistency two extracts prepared from independent biological experiments were analysed in pairs.

2.7. Immunodetection

APX, GR and CAT were immunodetected after denaturing gel electrophoresis and Western-blotting (Laemmli 1970), using α -cytosolic APX (AS06180), α -GR (AS06181) and α -CAT (AS152991) (Agrisera, Vännäs, Sweden). After electrophoresis (20 μ g total protein), they were blotted onto a nitrocellulose membrane (BioTraceNT Pall Corporation, East Hills, NY, USA) using a semi-dry procedure (Trans Blot SD Semi-Dry Electrophoretic Transfer Cell, BioRad). Gel slabs were incubated in transfer buffer (48 mM Tris-HCl, 39 mM glycine, 1.3 mM SDS, and 20% methanol at pH 8.3) and then electroblotted for 1 h. The membrane was blocked with 1% bovine serum albumin in Tris-buffer-saline (TBS), and incubated overnight at 4°C with the primary antibodies diluted 1/2000. After several washes with TBS, membranes were incubated with the secondary antibody (α -rabbit IgG goat:horseradish peroxidase, Ref. A00160, GenScript, Piscataway, NJ, USA) diluted 1/10.000 for 2 h. Proteins were detected by incubating with LumiSensor™ Chemiluminescent HRP Substrate Kit (Ref. L00221V300, GenScript), and images taken with ChemiDoc™ XRS+ System (BioRad). Two extracts prepared from independent biological experiments were analysed in pairs by means of data consistency.

2.8. Statistical analysis

Three to four analytical replicates were measured of three independent biological experiments, and data were subjected to one-way ANOVA statistical analysis with post-hoc Duncan test using SPSS 17.0 (SPSS Inc., Chicago, USA). Results were expressed as mean plus standard error, and differences were considered significant at $p < 0.05$.

3. Results

3.1 Microalgae growth and aluminium toxicity

Growth of *Scenedesmus obliquus* was not affected significantly by pH, which concurs with the known tolerance of this microalgae to acidic growth conditions (Hodaifa et al., 2009). Therefore, *Scenedesmus* could be grown at acidic pH, which was more favourable to maintain Al in a soluble chemical form. In addition, microalgal biomass was similar at the different Al doses in the culture

medium (Fig. 1A), but we could observe that cells tended to form clumps, especially at the highest Al dose (100 μ M) when flasks rotary movement stopped. Close microscopic analysis revealed that increasing Al concentration lead to greater cell aggregation, as observed in bright field and chlorophyll autofluorescence imaging, thus large masses of cells were detected at the highest concentration of Al in the culture medium (Fig. 1B). Under control conditions, *Scenedesmus obliquus* showed characteristic bicellular colonies with propping spikelets, but under Al stress colonies became multicellular and numerous clumps were observed, while chlorophyll fluorescence help to distinguish chloroplasts of cells from other particulate material that could be present in the masses formed under Al stress (Fig. 2A). On the other hand, there were cell ultrastructural alterations caused by Al, as lipid corpuscles (green arrowheads) and autophagy-like vesicles (red arrowheads) appeared under 10 μ M Al exposed microalgae (Fig. 2C). Similar changes were observed under 100 μ M Al, ease to detect autophagy vesicles, scattered white starch granules, and also granulated extracellular material that could be involved in the multicellular aggregation observed (blue asterisk, Fig. 2D). The nature of the extracellular material that promotes formation of cellular clumps is unknown, but the precipitates were not disrupted by treating the cells with plant cell wall glucanases or proteases (trypsin) (data not shown), although some kind of polymeric exudate may appear in *Scenedesmus* (Salim et al., 2011).

The moderate effect of Al on *Scenedesmus* biomass was reflected also on chlorophyll concentration that did not change significantly (Fig. 3A), or even trend to increase slightly, implying that in our experimental conditions cells did not suffer acute stress. On the other hand, lipid peroxidation increased in *Scenedesmus* exposed to 100 μ M Al reached values that almost doubled those measured in control cells (Fig. 3B). Thus, to confirm that high dose of Al lead to oxidative stress induction we incubated cells with H₂DCFDA, fluorescent probe used frequently to monitor H₂O₂ and organic peroxides formed in cells suffering from redox imbalance (Ortega-Villasante et al., 2016), which fluorescence was measured in a titer plate reader. As shown in Fig. 3C, *Scenedesmus* subjected to 100 μ M Al stress suffered from oxidative stress, since H₂DCFDA fluorescence increased gradually with time of incubation. However, fluorescence values remained much lower in control cells or exposed to 10 μ M Al (approximately 8-times lower; Fig. 3C). In consequence, *Scenedesmus* showed clear oxidative stress symptoms, which prompted us to study the responses of antioxidant enzymes known to control the cellular levels of ROS.

Analysis of Al concentration in *Scenedesmus* sp. cells revealed its accumulation following the dose given, about one order of magnitude larger in 100 μ M Al-treated microalgae than in 10 μ M Al exposed ones (Fig. 4). Therefore, despite complex chemical equilibria of Al species in solution, Al was sufficiently bioavailable to be accumulated at large quantities in *Scenedesmus* cells cultivated in BBM growth media at pH 5.0. We also determined the concentration of several important macro and micronutrients such as Ca, Mg, Fe and Zn. Ca and Zn showed the strongest effects upon Al treatment, with a significant diminution respectively of 40 and 60% (Fig. 4). On the other hand, Mg and Fe only decreased by about 20 and 10%, respectively.

3.2 Antioxidant response under aluminium stress

We used ND-PAGE electrophoresis to analyse APX, CAT, SOD and GR *in gel* activities, technique that allows identification of putative changes in activity of particular isoforms under Al stress. Thus, remarkable changes in antioxidant activities were found in *Scenedesmus* provided with control, 10 and 100 μ M Al (Fig. 5). There was a gradual loss of APX and CAT activities under Al stress, specifically remarkable at 100 μ M Al. These enzymes are known to scavenge excess H_2O_2 generated under oxidative stress, which may be related with the accumulation of ROS under that Al treatment (Fig. 3C). Similarly, the activity of three detected SOD isoforms, MnSOD, Cu/ZnSOD and FeSOD, decreased concomitantly as Al concentration increased, with almost complete inhibition at 100 μ M Al. Therefore, these results imply that Al caused a dose-related inhibition of antioxidant enzymes directly involved in attenuation of ROS accumulation. On the other hand, *Scenedesmus* GR activity decreased slightly at 10 μ M Al, but exhibited a remarkable rise when exposed to 100 μ M A. This enzyme is particularly important to maintain the cellular redox balance promoting the reduction of glutathione (Hernández et al., 2015).

Due to the changes found in antioxidant enzyme activities, we analysed possible effects of Al stress on protein abundance using specific polyclonal antibodies α -cytosolic APX, α -CAT and α -GR for immunodetection after denaturing PAGE. Although reactivity of plant-derived α -APX antibody was low towards *Scenedesmus* APX, Al stress clearly led to lower accumulation of APX particularly at 100 μ M Al (Fig. 6). Similar pattern was observed for GR, which abundance decreased concomitantly at the highest concentration of Al in the culture medium. On the other hand, CAT showed a completely different behaviour, since apparently low level of the enzyme

was detected in control and 10 μM Al-exposed cells, to accumulate intensely when metal concentration increased to 100 μM Al (Fig. 6).

4. Discussion

Several aluminium salts are used as flocculation reagents to allow pre-concentration of microalgae used for water recycling and treatment, which allows subsequent efficient harvesting by filtration or centrifugation to obtain valuable dehydrated biomass (Rwehumbiza et al., 2012). In particular, water soluble Al salts, like aluminium sulphate ($\text{Al}_2(\text{SO}_4)_3$), were used at high concentrations (0.5 to 1 mM) to flocculate efficiently *Scenedesmus obliquus* by means of biomass harvesting (Rhea et al., 2017). Aluminium oxide nanoparticles (Al_2O_3), which are regularly used for water treatment, produced a strong aggregation when *Scenedesmus* and *Chlorella* microalgae were exposed to doses above 100 μM (Sadiq et al., 2011). *Scenedesmus* cells also aggregated and formed multicellular colonies and aggregates when subjected to Cu, Cd and Cr stress (Peña-Castro et al. 2004), or exposed to Zn nanoparticles (Bhuvaneshwari et al., 2015). On the other hand, *Scenedesmus* has the ability to self-aggregate under certain growth conditions, such as nutrient deprivation, possibly by the secretion of extracellular substances (Salim et al., 2011). Aggregation may be part of a protection mechanism under stressful conditions, which leads to multicellular colonies, characteristic of *Scenedesmus* species (Lürling, 2003). Therefore, the observed aggregation of cells under Al stress found in *Scenedesmus* (Fig. 1 and 2) seems a conserved response, which may contribute to cell survival under harmful growth conditions. In fact, Al did not affect significantly *Scenedesmus* biomass production (Fig. 1), in agreement with reported tolerance of *Scenedesmus acutiformis* to Cd cultivated under comparable growth conditions (Kováčik et al., 2017). Several marine diatoms strains suffer toxicity to soluble Al chemical species (prepared from AlCl_3) at concentrations well above 100 μM , which growth and membrane permeability were negatively affected, while cells trend to precipitate (Gillmore et al., 2016). Similar tolerance to metals was observed in microalgae like *Chlamydomonas reinhardtii*, which cell growth was only hampered under high concentrations of Cd (100 to 200 μM) in short-term experiments equal to those performed here (Samadani et al., 2018).

Cytotoxic symptoms appeared at the subcellular ultrastructure, with proliferation of autophagy vesicles, deposition of lipid bodies and appearance of white starch granules in *Scenedesmus* cells treated with Al (Fig. 2). Similar alterations appeared in *Chlorella* cells exposed

to Al₂O₃ nanoparticles (at 20 µM Al concentration), with numerous starch grains and autophagy-like vesicles (Pakrashi et al. 2013). Additionally, *Chlorella* cells showed distorted shapes and abnormal cell wall structures with few adhered Al₂O₃ nanoparticles, as could be observed by electron scanning microscopy (Sadiq et al., 2011; Pakrashi et al. 2013). Cellular ultrastructure modifications look as if are common response of microalgae to metal stress, such occurred in *Scenedesmus armatus* grown in the presence of Cd (Tukaj et al., 2007), *Micrasterias denticulate* under Cr stress (Volland et al., 2012), *Chlamydomonas reinhardtii* exposed to Cd (Samadani et al., 2018), or *Ankistrodesmus falcatus* treated with Ni (Martínez-Ruiz and Martínez-Jerónimo 2015). Therefore, our results indicate that Al promotes cellular damages similar to those observed under stress induced by various toxic metals, possibly by altering common physiological processes like carbon and lipid metabolism.

Remarkable depletion of Ca and Zn appeared in cells treated with 100 µM Al (Fig. 4). Similar negative effect on Ca accumulation was described in *Scenedesmus* exposed to another toxic elements like Cd, Ni, Pb and Hg (Kováčik et al., 2017; 2018). Calcium is an important inorganic component of microalga cell walls, which binds to acidic cellular components similar to pectins (Baudeflet et al., 2017). Therefore, lower Ca incorporation to *Scenedesmus* may result in altered cell shape, as that observed under 100 µM Al (Fig. 3D). Interestingly, Kováčik and Dresler (2018) showed that elevated doses of Ca prevented toxic effects of Cd, Mn and Pb despite accumulation of those metals was not affected. It is feasible to assume that displacement of Ca from cellular components by toxic metals may result in several damage symptoms. On the other hand, Zn is an essential micronutrient that is important to maintain photosynthesis, protein stabilisation and antioxidant responses in microalgae (Malasam et al., 2013), processes that may be at stake due to Al-induced Zn starvation. In overall, poor accumulation of nutrients, as those observed under Al in *Scenedesmus* (Fig. 4), may reflect general alteration of cell membranes integrity, as Al is known to inhibit plasmalemma H⁺-ATPase and block active membrane transport processes (Ma, 2007).

The above-mentioned cell alterations due to Al exposure results frequently in the onset of oxidative stress. For example, oxidative stress appeared in BY2 tobacco cells provided with Al₂O₃ nanoparticles, which resulted in ROS accumulation and enhanced lipid peroxidation (Poborilova et al., 2013). In fact, lipid peroxidation was an early toxic symptom occurring in pea and soybean roots exposed to Al (Cakmak and Horst, 1991). Remarkably, we found strong lipid peroxidation

induction in *Scenedesmus* treated with 100 μM Al (Fig. 3B), in a similar manner as was found in two cyanobacteria species treated with 100 and 200 μM Al (Hamed et al., 2019). Aluminium also led to the generation of ROS in *Lotus corniculatus* and maize epidermal cells (Navascués et al., 2011; Jones et al., 2006), which were associated with cell wall deformation and root growth inhibition. These results concur with the strong induction of H₂DCFDA fluorescence caused by ROS accumulation in *Scenedesmus* exposed to 100 μM Al (Fig. 3C), response also described in *Chlorella* (Pakrashi et al., 2013). H₂DCFDA fluorescence increase upon Al treatment closely resembles the data collected by Kováčik et al. (2015) and Kováčik et al. (2017) in *Scenedesmus* subjected to Cr and Cd stress, which imply that one of the toxic effects of Al is the promotion of redox cellular imbalance.

Metal induced oxidative stress is a consequence of ROS accumulation and inefficient antioxidant machinery, which is unable of limiting ROS production (Cuypers et al., 2016). Antioxidant enzymes like APX, CAT, SOD and GR are considered key components to maintain ROS levels under control (Foyer and Noctor, 2005). Although there are controversial data in the literature, depending on metal chemical properties and the experimental conditions, the cellular redox balance is compromised by altering the activity of antioxidant enzymes (Hernández et al., 2015). In this sense, our results show in *Scenedesmus* cells a limited inhibition of SOD, CAT APX and GR activities under 10 μM Al, but a strong inhibition of SOD, CAT and APX activities when exposed to 100 μM Al, while GR activity clearly increased under this condition (Fig. 5). On the contrary, CAT activity increased in *Anabaena* cyanobacteria treated with 100 to 200 μM Al, whereas other antioxidant enzymes (i.e. APX or GR) had modest activation (Hamed et al., 2019). Aluminium toxicity also caused differential responses of antioxidant enzymes in *Lotus corniculatus* roots, with strong inhibition of Cu/ZnSOD and dehydroascorbate reductase, not apparent changes in the activity of APX and GR, whereas FeSOD activity was greater (Navascués et al., 2011). It seems that SODs are particularly sensitive to metal toxicity, since SOD activity was remarkably inhibited in the *Chlorella vulgaris* marine microalgae treated with ZnO nanoparticles (Suman et al., 2015), and in *Scenedesmus acutiformis* exposed to Cd (Kováčik et al., 2017). In the opposite, *Scenedesmus* CAT activity was strongly induced upon Cd stress, whereas APX did not change appreciably (Kováčik et al., 2017). However, similar inhibitory effects of Al on APX and CAT as observed in *Scenedesmus* (Fig. 5) were found in roots of potato plantlets, which activities decreased remarkably as Al doses increased (Tabaldi et al., 2009). In addition,

SOD, CAT and APX activities showed a characteristic hormetic response to Al in cucumber seedlings, peaking at 10 to 100 μM Al, but decreasing to values below controls at doses above 1000 μM Al (Pareira et al., 2010). Comparable hormetic response was found in the microalga *Gonyaulax polyedra* exposed to toxic metals Hg, Cd, Pb, and Cu, with significant inhibition of SOD and APX activities under acute stress conditions (Okamoto et al., 2001). Finally, GR activity increased clearly in *Scenedesmus* treated with 100 μM Al (Fig. 5), following a similar response as that found under Cd stress (Kováčik et al., 2017). On the contrary, *Scenedesmus* GR activity was sensitive to Cu (10 μM) and Zn (25 μM), falling up to 50% of control values (Tripathi et al., 2006), or at concentrations above 50 μM Cu, which correlated with enlarged levels of H_2O_2 (Nagalakshmi and Prasad 2001). To sum up, several plants and microalgae organisms exposed to different metal treatments experienced significant alterations in antioxidant enzymes, frequently resulting in activity inhibition of key antioxidant enzymes known to contribute to the control of the cellular redox balance. Such negative effects of metals may explain, at least partially, the building of ROS and oxidative stress, as those detected in *Scenedesmus* under Al stress (Fig. 3).

In order to explore whether the changes induced by Al in the activity of antioxidant enzymes were due to changes in enzyme levels, we analysed the levels of APX, CAT and GR by immunodetection after Western-blotting (Fig. 6). APX levels decreased as Al concentration was higher, which could explain the depletion detected of this enzymatic activity. However, CAT amount peaked at the highest dose of Al (Fig. 6), in opposition to the strong inhibition of its enzymatic activity (Fig. 4). The opposite occurred with the levels of GR, which amount clearly depleted at the highest dose of Al (Fig. 6), whereas GR activity increased (Fig. 4). The same pattern observed for CAT in *Scenedesmus* cells appeared in pea leaves exposed to 50 μM Cd, where CAT activity was significantly inhibited but CAT gene expression increased (Romero-Puertas et al., 2007). Interestingly, Cu excess (doses above 100 μM) also caused a remarkable inhibition of CAT activity in *Chlamydomonas reinhardtii*, whereas CAT expression almost triplicated control levels at 200 μM Cu, while SOD activity and expression did not change appreciably (Luis et al., 2006). Incidentally, inhibition of CAT activity caused by Cd in tobacco seedlings was counteracted by the over expression of *Brassica juncea* CAT3 gene encoding CAT3 isoform, which resulted in the attenuation of oxidative stress symptoms (Guan et al., 2009). Thus, it is feasible CAT is inhibited by a post-translational mechanism, that prevents reposition of enzymatic activity despite the strong induction of protein expression. In this sense, although some enzymes are overexpressed under Al

stress, such as CAT, activity that may be compromised by displacement of metal cofactors or improper protein folding (DalCorso et al., 2013). To sum up, specific and differential responses were detected between the studied redox enzymes, which is a common feature of antioxidant enzymatic activity under metal stress (Hernández et al., 2015). In consequence, exposure to Al may affect the activity of critical antioxidant enzymes, which may explain at least partially the symptoms of oxidative stress observed in *Scenedesmus*.

5. Conclusion

Scenedesmus suffered oxidative stress symptoms induced by Al, probably associated with the strong inhibition of antioxidant enzymes such as CAT, different SOD isoforms and APX. In some cases, cells responded to compensate that loss of activity, but was insufficient to restore the compromised redox balance caused by high concentrations of Al. Cytotoxic effects were observed as cells tend to aggregate and remarkable cell ultrastructure alterations were detected, where depletion of Ca and other nutrients may contribute accordingly. Several physiological parameters can be proposed as biomarkers of Al toxicity, such as H₂DFCDA fluorescence or strong inhibition of CAT, both easy to detect at cellular or biochemical levels. Future work should focus to understand the homeostatic mechanisms to cope with Al toxicity, which may help to optimize tolerance of microalgae to this hazardous metal.

AUTHOR DECLARATION

We wish to confirm that there are no known conflicts of interest associated with this publication and there has been no significant financial support for this work that could have influenced its outcome.

6. Acknowledgements

This research was supported by Spanish MICINN, through Projects AGL2014-53771-R and AGL2017-87591-R. Kharazmi University of Tehran provided an internship grant to M.A. to complete her experiments at Universidad Autónoma Madrid.

References

- Avami, A., Sattari, S., 2007. Energy conservation opportunities: cement industry in Iran. *Int. J. Energy* 1, 65-71.
- Bache, B. W., 1986. Aluminium mobilization in soils and waters. *J. Geol. Soc.* 143, 699-706.
- Baudelet, P-H., Ricochon, G., Linder, M., Muniglia, L., 2017. A new insight into cell walls of Chlorophyta. *Algal Res.* 25, 333-371.
- Bhuvaneshwari, M., Iswarya V., Archanaa, S., Madhu, G.M., G.K. Suraish-Kumar, G.K., Nagarajan, R., Chandrasekaran, N., Mukherjee, A., 2015. Cytotoxicity of ZnO NPs towards fresh water algae *Scenedesmus obliquus* at low exposure concentrations in UV-C, visible and dark conditions. *Aquat. Toxicol.* 162, 29–38.
- Beauchamp, C., Fridovich, I., 1971. Superoxide dismutase: improved assays and an assay applicable to acrylamide gels. *Anal. Biochem.* 44, 276-287.
- Bold, H. C., 1949. The morphology of *Chlamydomonas chlamydogama*, sp. nov. *Bull. Torrey Bot. Club*, 101-108.
- Cakmak, I., Horst, W. J., 1991. Effect of aluminium on lipid peroxidation, superoxide dismutase, catalase, and peroxidase activities in root tips of soybean (*Glycine max*). *Physiol. Plantarum*, 83, 463-468.
- Christenson, L., Sims, R., 2011. Production and harvesting of microalgae for wastewater treatment, biofuels, and bioproducts. *Biotechnol. Adv.* 29, 686-702.
- Choudhary, M., Jetley, U. K., Khan, M. A., Zutshi, S., Fatma, T., 2007. Effect of heavy metal stress on proline, malondialdehyde, and superoxide dismutase activity in the cyanobacterium *Spirulina platensis*-S5. *Ecotoxicol. Environ. Safety* 66, 204-209.
- Cuyper, A., Hendrix, S., Amaral dos Reis, R., De Smet, S., Deckers, J., Gielen, H., Jozefczak, M., Loix, C., Hanne Vercampt, H., Vangronsveld, J., Keunen, E., 2016. Hydrogen peroxide, signaling in disguise during metal phytotoxicity. *Front. Plant Sci.* 7, 470.
- DalCorso, G., Manara, A., Furini, A., 2013. An overview of heavy metal challenge in plants: from roots to shoots. *Metallomics*, 5, 1117-1132.

- Delhaize, E., Ryan, P. R., 1995. Aluminum toxicity and tolerance in plants. *Plant Physiol.* 107, 315-321.
- Danilov, R. A., Ekelund, N. G., 2002. Effects of short- term and long- term aluminium stress on photosynthesis, respiration, and reproductive capacity in a unicellular green flagellate (*Euglena gracilis*). *Acta Hydrochim. Hydrobiol.* 30, 190-196.
- Fischer, B.B., Wiesendanger, M., Eggen, R.I.L., 2006. Growth condition-dependent sensitivity, photodamage and stress response of *Chlamydomonas reinhardtii* exposed to high light conditions. *Plant Cell Physiol.* 47, 1135–1145.
- Foyer, C.H., Noctor, G., 2005. Redox homeostasis and antioxidant signalling: a metabolic interface between stress perception and physiological responses. *Plant Cell* 17, 1866-1875.
- Gao BY, Yue Q, Wang B., 2004. Coagulation efficiency and residual aluminum content of polyaluminum silicate chloride in water treatment. *Acta Hydrochim. Hydrobiol.* 32:125–30.
- Gillmore, M. L., Golding, L. A., Angel, B. M., Adams, M. S., Jolley, D. F., 2016. Toxicity of dissolved and precipitated aluminium to marine diatoms. *Aquat. Toxicol.* 174, 82-91.
- Guan, Z., Chai, T., Zhang, Y., Xu, J., Wei, W., 2009. Enhancement of Cd tolerance in transgenic tobacco plants overexpressing a Cd-induced catalase cDNA. *Chemosphere*, 76, 623-630.
- Gustafsson, J. P., 2014. Geochemical equilibrium speciation model Visual MINTEQ Ver. 3.1. KTH, Department of Land and Water Resources Engineering, Stockholm, Sweden.
- Hamed, S. M., Hassan, S. H., Selim, S., Kumar, A., Khalaf, S. M., Wadaan, M. A., Hozzein, W.N., Abdelgawad, H., 2019. Physiological and biochemical responses to aluminum-induced oxidative stress in two cyanobacterial species. *Environ. Poll.* 251, 961-969.
- Haydar, S., Aziz, J. A., 2009. Coagulation–flocculation studies of tannery wastewater using combination of alum with cationic and anionic polymers. *J. Hazard. Mat.* 168, 1035-1040.
- Hernández, L. E., Sobrino-Plata, J., Montero-Palmero, M. B., Carrasco-Gil, S., Flores-Cáceres, M. L., Ortega-Villasante, C., Escobar, C., 2015. Contribution of glutathione to the control of cellular redox homeostasis under toxic metal and metalloid stress. *J. Exp. Bot.* 66, 2901-2911.

- Hodaifa, G., Martínez, M.E., Sánchez, S., 2009. Influence of pH on the culture of *Scenedesmus obliquus* in olive-mill wastewater. *Biotechnol. Bioproc. Eng.* 14, 854-860.
- Howe, G., Merchant, S., 1992. Heavy metal-activated synthesis of peptides in *Chlamydomonas reinhardtii*. *Plant Physiol.* 98, 127-136.
- Hu, C., Liu, H., Qu, J., Wang, D., Ru, J., 2006. Coagulation behavior of aluminum salts in eutrophic water: significance of Al₁₃ species and pH control. *Environ. Sci. Tech.* 40, 325-331.
- Huntzinger, D. N., Eatmon, T. D., 2009. A life-cycle assessment of Portland cement manufacturing: comparing the traditional process with alternative technologies. *J. Cleaner Product.* 17, 668-675.
- Huynh, V.B., Repellin, A., Zuily-Fodil, Y., Pham-Thi, A.T., 2012. Aluminum stress response in rice: effects on membrane lipid composition and expression of lipid biosynthesis genes. *Physiol. Plant.* 146, 272-284.
- Jones, D.L., Blancaflor, E.B., Kochian, L.V., Gilroy, S., 2006. Spatial coordination of aluminium uptake, production of reactive oxygen species, callose production and wall rigidification in maize roots. *Plant Cell Environ.* 29, 1309-1318.
- Kováčik, J., Bujdoš, M., Babula, P., 2018. Impact of humic acid on the accumulation of metals by microalgae. *Environ. Sci. Poll. Res.* 25, 10792-10798.
- Kováčik, J., Dresler, S., 2018. Calcium availability but not its content modulates metal toxicity in *Scenedesmus quadricauda*. *Ecotox. Environ. Safety* 147, 664-669.
- Kováčik, J., Babula, P., Peterková, V., Hedbavny, J., 2017. Long-term impact of cadmium shows little damage in *Scenedesmus acutiformis* cultures. *Algal Res.* 25, 184-190.
- Kováčik, J., Babula, P., Hedbavny, J., Kryštofová, O., Provazník, I., 2015. Physiology and methodology of chromium toxicity using alga *Scenedesmus quadricauda* as model object. *Chemosphere* 120, 23-30.
- Kumar, K.S., Dahms, H.U., Won, E.J., Lee, J.S., Shin, K.H., 2015. Microalgae—A promising tool for heavy metal remediation. *Ecotoxicol. Environ. Safety* 113, 329-352.

- Laemmli, U.K., 1970. Cleavage of structural proteins during the assembly of the head of bacteriophage T4. *Nature* 227, 680–685.
- Lee, H., Suh, J.H., Kim, I.B., Yoon, T., 2004. Effect of aluminum in two-metal biosorption by an algal biosorbent. *Miner. Eng.* 17, 487-493.
- Luis, P., Behnke, K., Toepel, J., Wilhelm, C., 2006. Parallel analysis of transcript levels and physiological key parameters allows the identification of stress phase gene markers in *Chlamydomonas reinhardtii* under copper excess. *Plant Cell Environ.* 29, 2043-2054.
- Lüring, M., 2003. Phenotypic plasticity in the green algae *Desmodesmus* and *Scenedesmus* with special reference to the induction of defensive morphology. *Ann. Limnol. – Int. J. Lim.* 39, 85-101.
- Ma, J. F., 2007. Syndrome of aluminum toxicity and diversity of aluminum resistance in higher plants. *Int. Rev. Cytol.* 264, 225-252.
- Malasarn, D., Kropat, J., Hsieh, S. I., Finazzi, G., Casero, D., Loo, J. A., Pellegrini, M., Wollman, F-A., Merchant, S. S., 2013. Zinc deficiency impacts CO₂ assimilation and disrupts copper homeostasis in *Chlamydomonas reinhardtii*. *J Biol. Chem.* 288, 10672-10683.
- Martínez-Ruiz, E. B., Martínez-Jerónimo, F., 2015. Nickel has biochemical, physiological, and structural effects on the green microalga *Ankistrodesmus falcatus*: an integrative study. *Aquat. Toxicol.* 169, 27-36.
- Miazek, K., Iwanek, W., Remacle, C., Richel, A., Goffin, D., 2015. Effect of metals, metalloids and metallic nanoparticles on microalgae growth and industrial product biosynthesis: A Review. *Int. J. Mol. Sci.* 16, 23929-23969.
- Mousavi, S. R., Balali-Mood, M., Riahi-Zanjani, B., Yousefzadeh, H., Sadeghi, M., 2013. Concentrations of mercury, lead, chromium, cadmium, arsenic and aluminum in irrigation water wells and wastewaters used for agriculture in Mashhad, northeastern Iran. *Int. J. Environ. Med.*, 4, 80-86.
- Nagalakshmi, N., Prasad, M., 2001. Responses of glutathione cycle enzymes and glutathione metabolism to copper stress in *Scenedesmus bijugatus*. *Plant Sci.* 160, 291-299.

- Navascués, J., Pérez-Rontomé, C., Sánchez, D.H., Staudinger, C., Wienkoop, S., Rellán-Álvarez, R., Becana, M., 2011. Oxidative stress is a consequence, not a cause, of aluminum toxicity in the forage legume *Lotus corniculatus*. *New Phytol.* 193, 625-636.
- Okamoto, O. K., Pinto, E., Latorre, L. R., Bechara, E. J. H., Colepicolo, P., 2001. Antioxidant modulation in response to metal-induced oxidative stress in algal chloroplasts. *Arch. Environ. Contam. Toxicol.* 40, 18-24.
- Oller, I., Malato, S., Sánchez-Pérez, J.A., 2011. Combination of advanced oxidation processes and biological treatments for wastewater decontamination-A review. *Sci. Total Environ.* 409, 4141-4166.
- Ortega-Villasante, C., Burén, S., Barón-Sola, Á., Martínez, F., Hernández, L. E., 2016. *In vivo* ROS and redox potential fluorescent detection in plants: Present approaches and future perspectives. *Methods* 109, 92-104.
- Ortega-Villasante, C., Rellán-Álvarez, R., del Campo, F.F., Carpena-Ruiz, R.O., Hernández, L.E., 2005. Cellular damage induced by cadmium and mercury in *Medicago sativa*. *J. Exp. Bot.* 56, 2239–2251.
- Pakrashi, S., Dalai, S., Prathna, T. C., Trivedi, S., Myneni, R., Raichur, A. M., Chandrasekaran, N., Mukherjee, A., 2013. Cytotoxicity of aluminium oxide nanoparticles towards fresh water algal isolate at low exposure concentrations. *Aquat. Toxicol.* 132, 34-45.
- Pereira, L.B., Mazzanti, C.M.A., Gonçalves, J.F., Cargnelutti, D., Tabaldi, L.A., Becker, A.G., Calgaroto, N.S., Gomes-Farias, J., Battisti, V., Bohrer, D., Nicoloso, F.T., Morsch, V.M., Schetinger, M.R.C., 2010. Aluminum-induced oxidative stress in cucumber. *Plant Physiol. Biochem.* 48, 683-689.
- Peña-Castro, J. M., Martínez-Jerónimo, F., Esparza-García, F., Cañizares-Villanueva, R. O., 2004. Phenotypic plasticity in *Scenedesmus incrassatulus* (Chlorophyceae) in response to heavy metals stress. *Chemosphere* 57, 1629-1636.
- Perales-Vela, H. V., Pena-Castro, J. M., Canizares-Villanueva, R. O., 2006. Heavy metal detoxification in eukaryotic microalgae. *Chemosphere* 64, 1-10.

- Poborilova, Z., Opatrilova, R., Babula, P., 2013. Toxicity of aluminium oxide nanoparticles demonstrated using a BY-2 plant cell suspension culture model. *Environ. Exp. Bot.* 91, 1-11.
- Poschenrieder, C., Gunsé, B., Corrales, I., Barceló, J., 2008. A glance into aluminum toxicity and resistance in plants. *Sci. Total Environ.* 400, 356-368.
- Ramazanov, Z., Rawat, M., Henk, M. C., Mason, C. B., Matthews, S. W., Moroney, J. V., 1994. The induction of the CO₂-concentrating mechanism is correlated with the formation of the starch sheath around the pyrenoid of *Chlamydomonas reinhardtii*. *Planta.* 195, 210-216.
- Romero-Puertas, M. C., Corpas, F. J., Rodríguez-Serrano, M., Gómez, M., Luis, A., Sandalio, L. M., 2007. Differential expression and regulation of antioxidative enzymes by cadmium in pea plants. *J. Plant Physiol.* 164, 1346-1357.
- Rhea, N., Groppo, J., Crofcheck, C., 2017. Evaluation of flocculation, sedimentation, and filtration for dewatering of *Scenedesmus* algae. *Transact. ASABE* 60, 1359-1367.
- Rugnini, L., Costa, G., Congestri, R., Bruno, L. 2017. Testing of two different strains of green microalgae for Cu and Ni removal from aqueous media. *Sci. Total Environ.* 601, 959-967.
- Rwehumbiza, V. M., Harrison, R., Thomsen, L., 2012. Alum-induced flocculation of preconcentrated *Nannochloropsis salina*: residual aluminium in the biomass, FAMES and its effects on microalgae growth upon media recycling. *Chem. Eng. J.* 200, 168-175.
- Sadiq, I.M., Pakrashi, S., Chandrasekaran, N., Mukherjee, A., 2011. Studies on toxicity of aluminum oxide (Al₂O₃) nanoparticles to microalgae species: *Scenedesmus* sp. and *Chlorella* sp. *J. Nanoparticle Res.* 13, 3287-3299.
- Salim, S., Bosma, R., Vetmuë, M.H., Wijffels, R.H., 2011. Harvesting of microalgae by bio-flocculation. *J. Appl. Phycol.* 23, 849-855.
- Samadani, M., Perreault, F., Oukarroum, A., Dewez, D., 2018. Effect of cadmium accumulation on green algae *Chlamydomonas reinhardtii* and acid-tolerant *Chlamydomonas* CPCC121. *Chemosphere* 191, 174-182.
- Siddique, R., 2006. Utilization of cement kiln dust (CKD) in cement mortar and concrete—an overview. *Resources Con. Recycl.* 48, 315-338.

- Sobrino-Plata, J., Ortega-Villasante, C., Flores-Cáceres, M. L., Escobar, C., Del Campo, F. F., Hernández, L. E., 2009. Differential alterations of antioxidant defenses as bioindicators of mercury and cadmium toxicity in alfalfa. *Chemosphere* 77, 946-954.
- Sloan, J.J., Basta, N.T., Westerman, R.L., 1995. Aluminum transformations and solution equilibria induced by banded phosphorus fertilizer in acid soil. *Soil Sci. Soc. Am. J.* 59, 357-364.
- Suman, T. Y., Rajasree, S. R., Kirubakaran, R., 2015. Evaluation of zinc oxide nanoparticles toxicity on marine algae *Chlorella vulgaris* through flow cytometric, cytotoxicity and oxidative stress analysis. *Ecotoxicol. Environ. Safety* 113, 23-30.
- Tabaldi L.A., Cargnelutti, D., Gonçalves, J.F., Belmonte-Pereira, L., Castro, G.Y. Maldaner, J., Rauber, R., Liana Verônica Rossato, L.V., Bisognin, D.A., Schetinger, M.R.C., Nicoloso, F.T., 2009. Oxidative stress is an early symptom triggered by aluminum in Al-sensitive. potato plantlets. *Chemosphere* 76, 1402–1409.
- Torricelli, E., Gorbi, G., Pawlik-Skowronska, B., Di Toppi, L. S., Corradi, M. G., 2004. Cadmium tolerance, cysteine and thiol peptide levels in wild type and chromium-tolerant strains of *Scenedesmus acutus* (Chlorophyceae). *Aquat. Toxicol.* 68, 315-323.
- Tripathi, B. N., Mehta, S. K., Amar, A., Gaur, J. P., 2006. Oxidative stress in *Scenedesmus* sp. during short-and long-term exposure to Cu^{2+} and Zn^{2+} . *Chemosphere* 62, 538-544.
- Tukaj, Z., Baścik-Remisiewicz, A., Skowroński, T., Tukaj, C., 2007. Cadmium effect on the growth, photosynthesis, ultrastructure and phytochelatin content of green microalga *Scenedesmus armatus*: A study at low and elevated CO_2 concentration. *Environ. Exp. Bot.* 60, 291-299.
- Volland, S., Andosch, A., Milla, M., Stöger, B., Lütz, C., Lütz Meindl, U., 2011. Intracellular metal compartmentalization in the green algal model system *Micrasterias denticulata* (streptophyta) measured by transmission electron microscopy–coupled electron energy loss spectroscopy. *J. Phycol.* 47, 565-579.
- Volland, S., Lütz, C., Michalke, B., Lütz-Meindl, U., 2012. Intracellular chromium localization and cell physiological response in the unicellular alga *Micrasterias*. *Aquat. Toxicol.* 109, 59-69.

Yamamoto, Y., Kobayashi, Y., Devi, S. R., Rikiishi, S., Matsumoto, H., 2002. Aluminum toxicity is associated with mitochondrial dysfunction and the production of reactive oxygen species in plant cells. *Plant Physiol.* 128, 63-72.

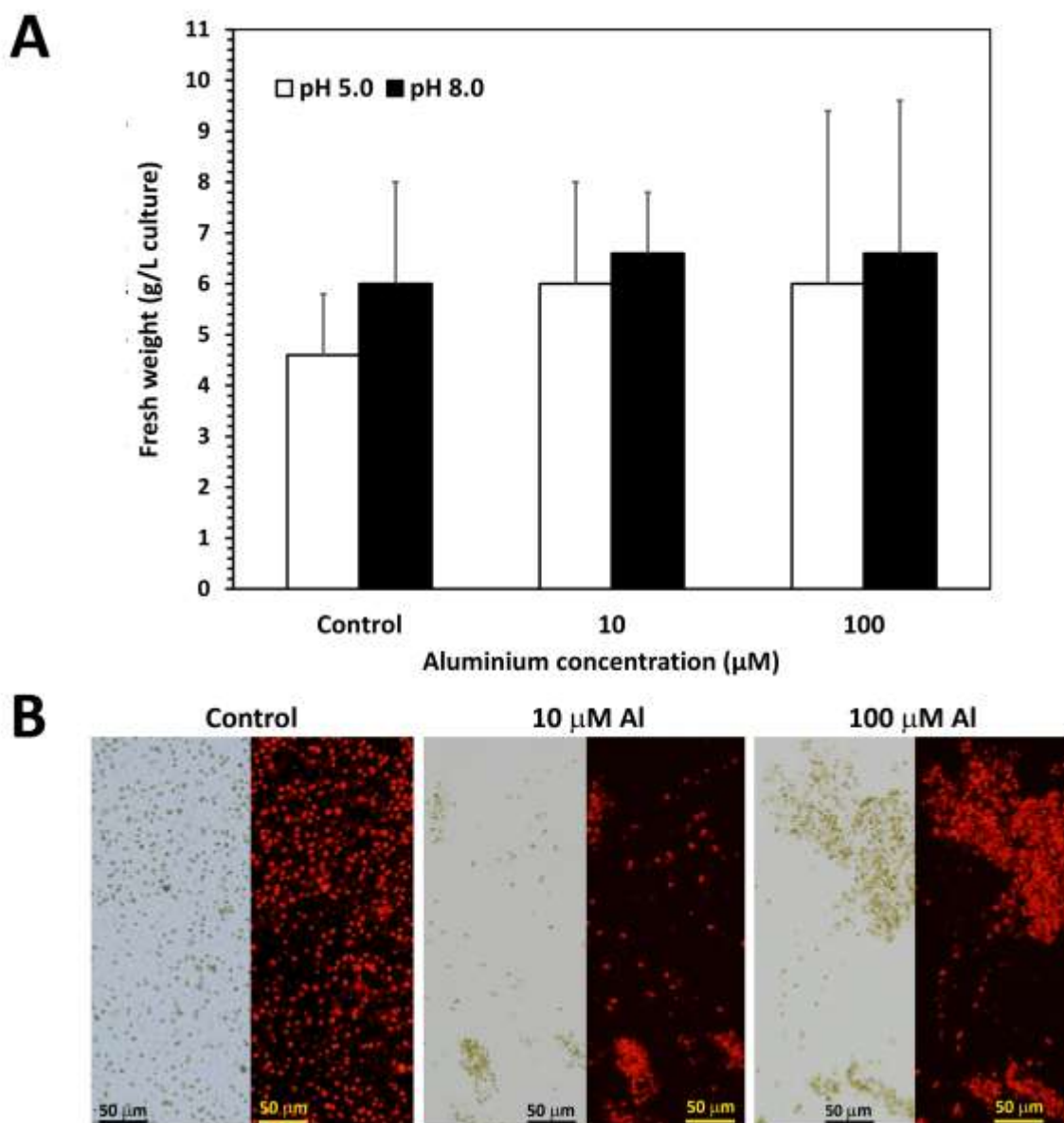


Figure 1. A) Fresh weight (g/L culture) of *Scenedesmus* sp. was not significantly affected by exposure to 0 (control), 10 and 100 μM Al in BBM/3 culture medium adjusted to pH 5 or 8 after 72 h. **B)** Visible image and chlorophyll autofluorescence taken of *Scenedesmus* cells to show aggregation occurring in the presence of Al in BBM/3 at pH 5.0.

Figure 2. A) Detail of *Scenedesmus* sp. aggregation occurring in the presence of Al, either in bright field and showing chlorophyll fluorescence. **B, C and D)** Transmission electron microscopy of cells treated for 72 h with 0 (control), 10 and 100 μ M Al in BBM/3 culture medium at pH 5.0, showing pyrenoid structures (p), thylakoids (t), characteristic spikelet (s), lipid corpuscles (green arrowhead), and autophagy-like vesicles (red arrowhead). Cells exposed to Al had starch granules detached from typical pyrenoid structures (purple arrowhead). The blue asterisk marks extracellular granular material found in the aggregates caused by 100 μ M Al exposure.

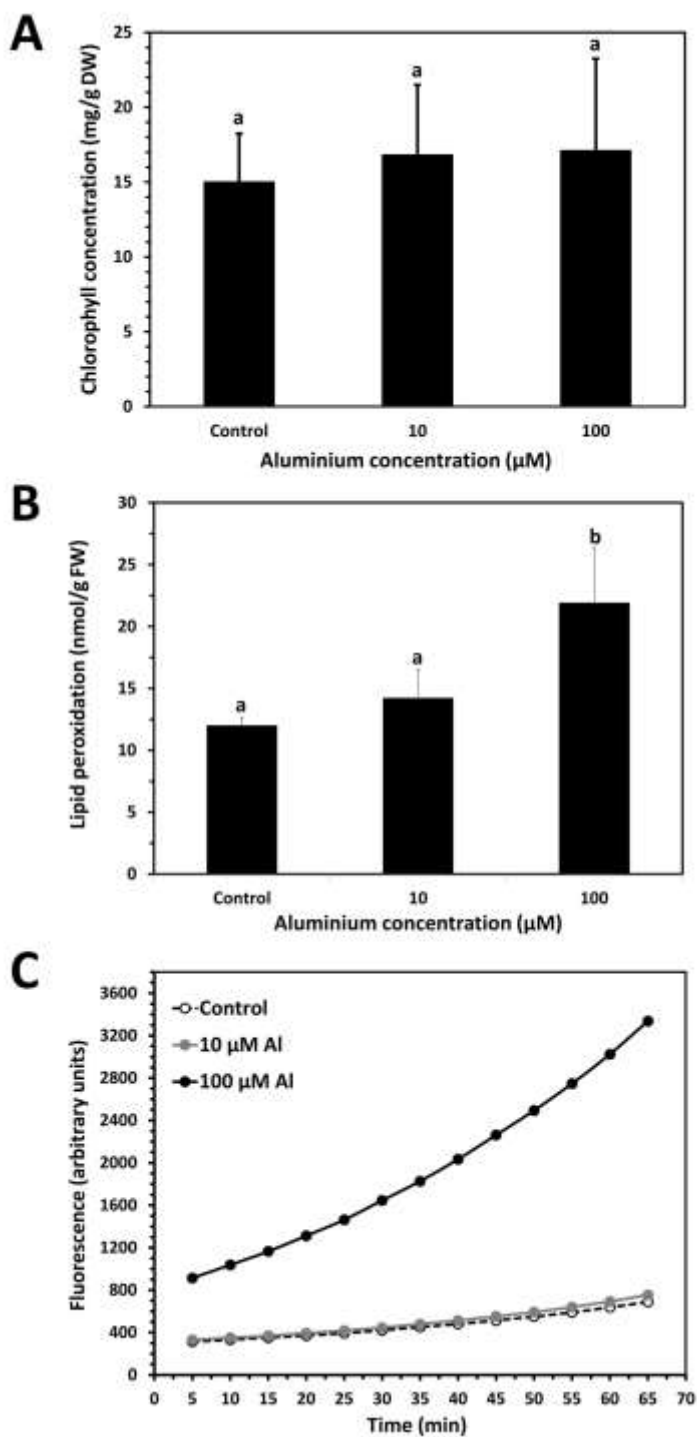


Figure 3. A) Chlorophyll concentration (mg/g DW), B) lipid peroxidation (nmol/g FW) and C) H₂DCFDA fluorescence as oxidative stress vital dye (arbitrary units of fluorescence) of *Scenedesmus* sp. treated for 72 h with 0 (control), 10 and 100 μ M Al in BBM/3 culture medium at pH 5.0. Different letters denote significant differences between treatments ($p < 0.05$). H₂DCFDA fluorescence standard deviation of eight replicates was below 5% in the experiment shown in panel C.

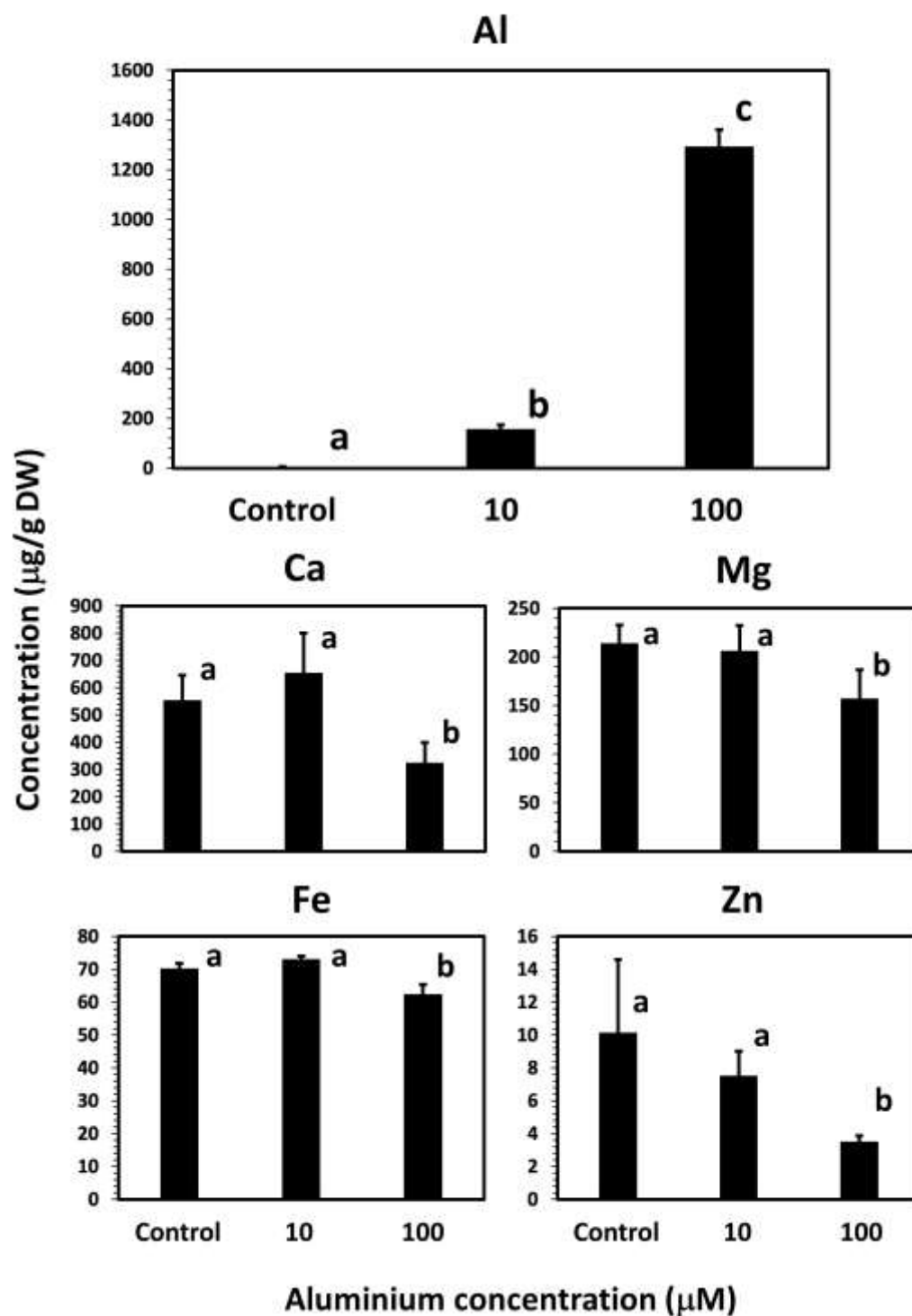


Figure 4. Concentration (µg/g DW) of Al, Ca, Mg, Fe and Zn in *Scenedesmus* sp. treated for 72 h with 0 (control), 10 and 100 µM Al in BBM/3 culture medium at pH 5.0. Different letters denote significant differences between treatments ($p < 0.05$).

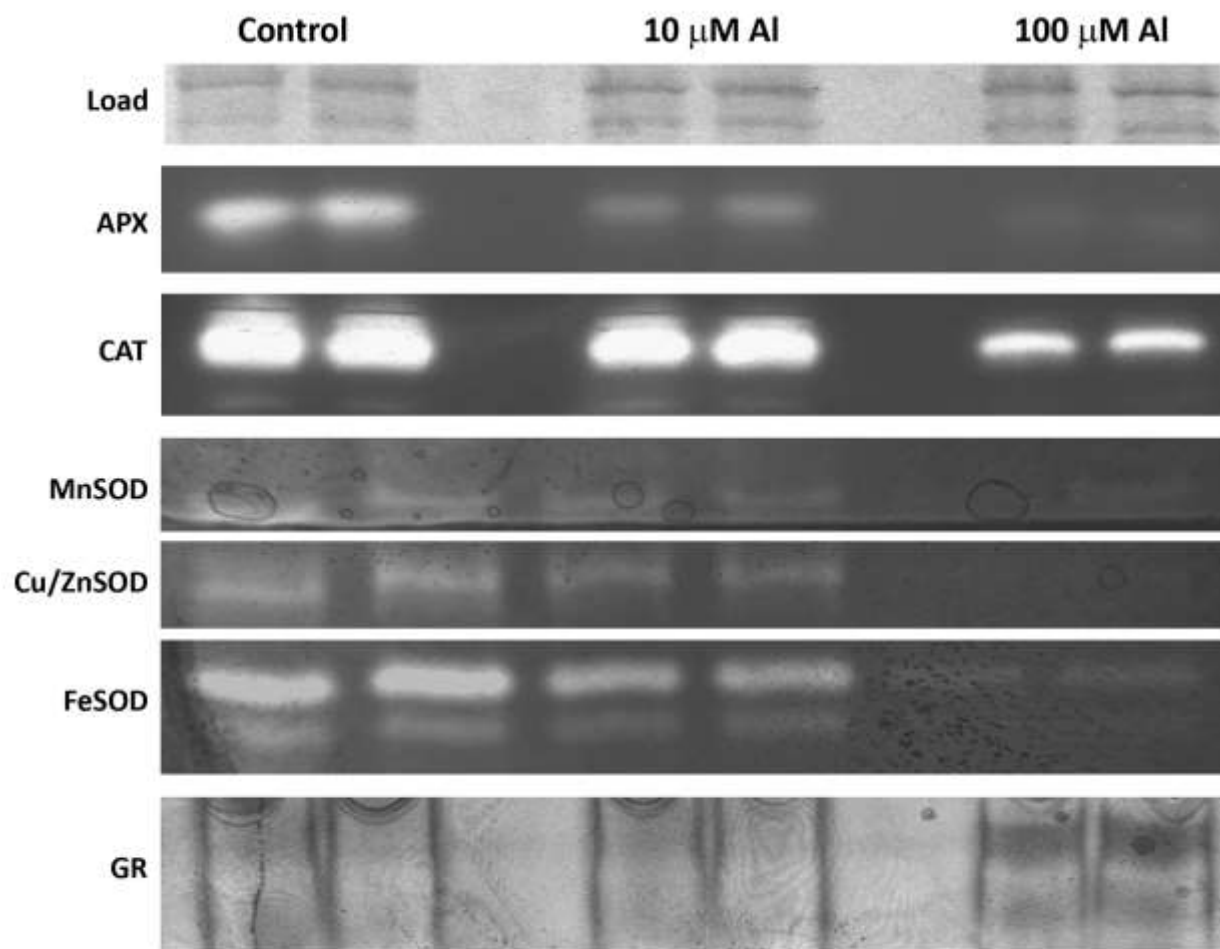


Figure 5. Representative antioxidant *in gel* activity after non-denaturing gel electrophoresis of two independent extracts is shown by means of consistency, prepared from *Scenedesmus* sp. treated with 0 (control), 10 and 100 μ M Al in BBM/3 culture medium for 72 h. Equal protein loading (15 μ g per sample) was checked using Coomassie blue general protein staining after denaturing gel electrophoresis (load). Figure shows ascorbate peroxidase (APX), catalase (CAT), superoxide dismutase (SOD) isoforms, and glutathione reductase (GR) activities.

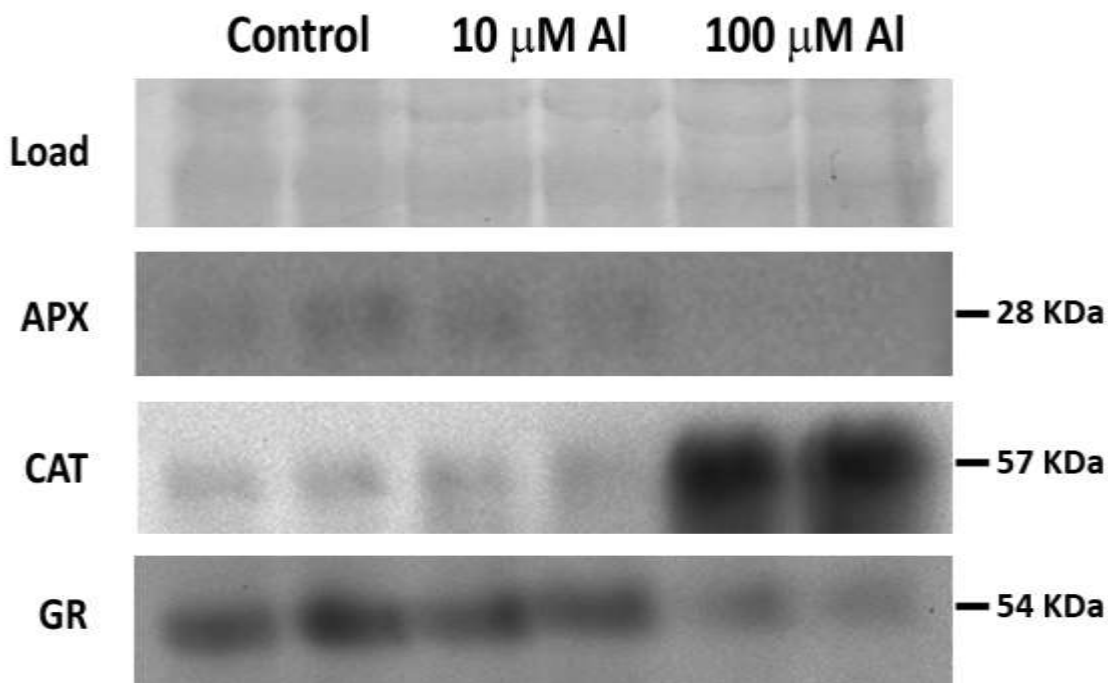


Figure 6. Representative Western-blot immunodetection of antioxidant enzymes after denaturing gel electrophoresis of two independent extracts is shown by means of consistency, prepared from *Scenedesmus* sp. treated with 0 (control), 10 and 100 μ M Al in BBM/3 culture medium for 72 h. Equal protein loading (15 μ g per sample) was checked using Coomassie blue general protein staining (load). Figure shows ascorbate peroxidase (APX), catalase (CAT), and glutathione reductase (GR) detection. On the right is shown the molecular weight (KDa) of bands detected, which corresponded with the expected size.

Table 1. Visual Minteq *in silico* Al speciation (%) in the Bold Basal Medium culture media containing EDTA or EDDHA (171.1 μM) as organic chelating reagents at pH 5.0 and 8.0.

	10 μM Al		100 μM Al		Chemical species
	pH 5.0	pH 8.0	pH 5.0	pH 8.0	
EDTA		0.2		0.2	$\text{Al}(\text{OH})_2\text{EDTA}^{3-}$
	90.9	1.0	90.9	1.0	AlEDTA^-
	8.7	98.8	8.7	98.8	$\text{Al}(\text{OH})\text{EDTA}^{2-}$
	0.4		0.4		AlHEDTA
EDDHA	1.7		1.8		Al^{3+}
	0.7		0.8		AlOH^{2+}
	0.3	0.1	0.4	0.1	$\text{Al}(\text{OH})_2^+$
	0.3		0.3		AlSO_4^+
	1.3		1.3		$\text{AlH}_2\text{PO}_4^{2+}$
	95.6		95.5		AlHPO_4^+
		99.3		99.3	$\text{Al}(\text{OH})_4^-$
		0.7		0.7	$\text{Al}(\text{OH})_3$ (AQ)